Comparison between AgriPV simulation and field data, soybean case

Ricardo N. de Castro[1], Victor E. C. Oliveira[1], Lucas Del Mouro[1]

[1]FIT Institute of Technology, Sorocaba (Brazil)

Abstract

This study evaluates the accuracy of an integrated radiative and crop-growth simulation framework for predicting soybean yields in Agrivoltaic (AgriPV) systems. Given global concerns about sustainable agriculture and renewable energy, accurately predicting crop yields under AgriPV conditions is critical. Using TMY-based irradiance data, geometric shading analysis, and crop physiological modeling, the study quantified Photosynthetically Active Radiation (PAR) availability and simulated biomass production during a summer cropping season. Results indicated PAR represented 40.93% of Global Horizontal Irradiance (GHI), reflecting significant photovoltaic module shading. Simulated yields differed by only 8.68% from measured field data, demonstrating strong correlation and validating the model's reliability. These findings confirm the developed radiative and crop modeling framework's applicability for AgriPV system planning, offering a robust tool for optimizing integrated energy-crop production while ensuring agricultural viability.

Keywords: Agrivoltaics, Radiative Modeling, Crop Modeling, PAR

1. Introduction

AgriPV integrates photovoltaic systems with agriculture, optimizing land use by generating solar energy alongside crop cultivation. While beneficial, photovoltaic module shading significantly influences crop growth and yields by altering radiation distribution. Precisely predicting Photosynthetically Active Radiation (PAR) availability is therefore crucial. This study compares simulated soybean yields, calculated through radiative decomposition models and geometric shading analyses combined with crop model equations with field data. The goal is to evaluate simulation accuracy and guide optimized AgriPV system designs.

2. Methodology

It used three different methodologies to build simulation, the first one regarding the modeling of radiation of the sun on AgriPV conditions, the second one for modeling of the crop yield in the same conditions and the third one obtain the field data and the comparison. The interconnection between the methodologies is shown on Figure 1 and the results of the Crop Models is compared with the field data.

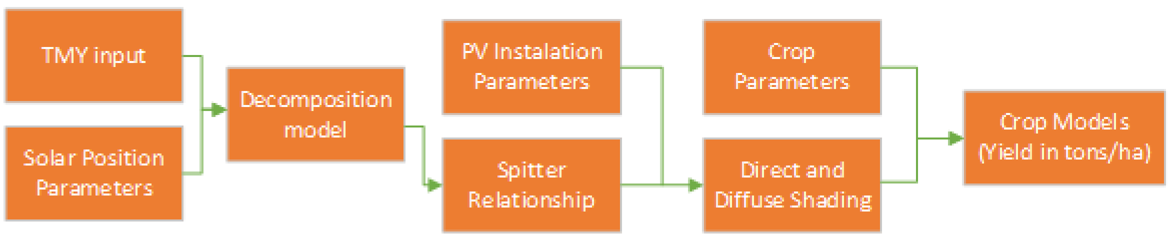

Fig. 1: Flowchart of the developed methodology

2.1. Radiative Modelling

Global Horizontal Irradiance (GHI) data from the Typical Meteorological Year (TMY) as in Huld et al (2018) is used as the primary input for radiative modeling and validated against locally measured data. The ENGERER2 model decomposes GHI into Diffuse Horizontal Irradiance (DHI) and Direct Normal Irradiance (DNI) as shown in Bright and Engerer (2019), while solar position parameters—including azimuth (ψ) and elevation (γ)—are calculated using standard astronomical algorithms to determine the solar incidence angle (θ) on inclined surfaces with pvlib implementation as in Anderson et al (2023). Photosynthetically Active Radiation (PAR), initially

10.18086/swc.2025.06.08 Available at http://proceedings.ises.org

estimated as 50% of GHI, is further separated into direct and diffuse components with the model shown in Spitters et al (1986), based on daily irradiation and average solar elevation. Shading from photovoltaic structures is addressed through binary modeling of direct shadows using geometric projections and through view factor calculations for diffuse radiation, quantifying sky obstruction, similarly as shown in Mikofski et al (2019). These adjustments yield corrected PAR values that accurately represent the radiation conditions experienced by crops under AgriPV systems.

TMY input and Solar Position Parameters

We used the PVGIS Typical Meteorological Year (TMY) via *pvlib.iotools.get_pvgis_tmy()* for Sorocaba, São Paulo. TMY is a synthetic year of 12 typical months, statistically selected from multi-year series, with hourly GHI/DNI/DHI data and meteorological variables. Irradiance comes from satellite products and the remaining variables from ERA reanalysis; the metadata indicates the years and database used in the composition. TMY represents the local average climate and is suitable for annual planning and simulations. To translate TMY irradiance to inclined planes/trackers, PVGIS uses the Muneer anisotropic model. Comparisons with alternative models and tower data show that this model is validated and there is no reason to replace it. In clear skies, typical relative errors are ≈4–6% for 1–10-minute data, and the report indicates better performance on an hourly basis. Therefore, we adopted the PVGIS TMY with the characteristic shown in Table 1 as a reliable basis for the annual simulations in this study based on the results shown on Gracia and Huld (2013).

Table 1: TMY metadata characteristics.

Characteristic	Information
Meteorological Data	PVGIS-SARAH3
Meteorological Database	ERA5
Horizon Database	DEM-calculated
Minimal Year Considered	2005
Maximal Year Considered	2023

We computed sun vectors with *pvlib.solarposition.get_solarposition()* for Sorocaba, São Paulo (−23.4239, −47.3649; 650 m; America/Sao_Paulo). The routine implements standard astronomical algorithms (NREL SPA in pvlib), returning apparent/true zenith and elevation, azimuth, and the equation of time. It is deterministic and does not rely on weather data. Inputs are time zone-aware timestamps; when not supplied, air pressure is inferred from altitude, with optional temperature/pressure to refine the atmospheric-refraction correction. These solar-position outputs drive our incidence-angle, shading geometry, and tracker kinematics, and ensure consistency with the tilt-plane transposition stage used alongside PVGIS so that geometry and irradiance modeling remain aligned at hourly resolution. Accordingly, we consider pvlib's solar-position calculations accurate for our application and fully compatible with the validated transposition framework employed in this study as the calculations is made as shown in Redas and Andreas (2004, 2007).

Decomposition model

Solar radiation is composed of direct and diffuse components, and how to decompose solar irradiance into its components is an important field of study. The direct component (Direct Normal Irradiance – DNI) is the energy emitted directly by the sun, defined as the ratio of the perpendicular incidence on a surface (eq. 3). The diffuse component (Diffuse Horizontal Irradiance – DHI) is the energy coming from other directions, given the scattering and reflection processes constituted by the atmosphere and neighboring surfaces and is defined relative to a horizontal surface (eq. 2). Combining both, we can define global irradiance (GHI) as the sum (eq. 1) and the DHI can be defined as the refollowing relation of the GHI and DNI.

$$GHI = DNI \times \cos(90^{\circ} - \gamma) + \mathrm{DHI} \quad \text{(eq. 1)}$$

$$DHI = Kd \times GHI \qquad \text{(eq. 2)}$$

$$DNI = \frac{GHI - Kd \times GHI}{\cos(90^{\circ} - \gamma)} \qquad \text{(eq. 3)}$$

The decomposition model of Engerer2 estimates the diffuse fraction K_d from GHI and astronomical-atmospheric predictors, producing DHI and DNI by balance closure and is shown in Engerer (2015). The model uses a globally reparametrized generalized logistic function for different temporal resolutions (1–60 min). The reported error of each temporal resolution is reported in Bright and Engerer (2019) and shown in the Table 2. The chosen temporal resolution on that work is 1-hour, to maintain the consistency with the TMY temporal resolution.

Table 2: Engerer2 reported error metrics.

Temporal average	RMSE	rRMSE (%)	MBE (%)	R^2
1-min	0.168	30.4	8.01	0.80
5-min	0.138	25.1	-0.30	0.86
10-min	0.136	24.8	-0.19	0.86
15-min	0.131	24.1	-0.08	0.87
30-min	0.125	23.2	0.01	0.88
1-hour	0.118	22.3	-0.04	0.89
1-day	0.183	33.1	3.80	0.46

The atmospheric predictors used in Engerer2 is defined as follow, where K_t is the clearness index (eq. 4), K_{tc} is the clear sky clearness index (eq. 5), ΔK_{tc} is the deviation between the previous indeces (eq. 6) and GHI_{cs} and GHI_{extra} is the global irradiance on a clear sky and in the extra-terrestrial situation. It's made an additional predictor (K_{de}) with the intention of capturing cloud-enhancements features (eq. 7).

$$K_t = \frac{GHI}{GHI_{extra}} \qquad \text{(eq. 4)}$$

$$K_{tc} = \frac{GHI_{cs}}{GHI_{extra}} \qquad \text{(eq. 5)}$$

$$\Delta \mathrm{K_{tc}} = \mathrm{K_{tc}} - \mathrm{K_t} \qquad \text{(eq. 6)}$$

$$K_{de} = \max\left(0, 1 - \frac{GHI_{cs}}{GHI}\right) \qquad \text{(eq. 7)}$$

The Engerer2 model takes the form of an adapted and generalized logistic function with a Kd estimator considered the time average of 1h as in (eq. 2) and calculated as in (eq. 8) with AST representing the apparent solar time.

$$\widehat{k_d} = -0.0097539 + \frac{1+0.0097539}{1+\exp(-5.3169+8.5084\times K_t + 0.013241\times AST + 0.0074356\times(90^{\circ}-\gamma) - 3.0329\Delta \mathrm{K_{tc}})} + 0.56403 \times K_{de} \qquad \text{(eq. 8)}$$

Spitter relationship

Photosynthetically active radiation (PAR, 400–700 nm) is initially approximated as half of the GHI. Subsequently, the diffuse fraction of PAR is derived using the Spitters et al. (1986) (eq. 9) relationship where k_d represents the daily diffuse fraction of global irradiance and is obtained with the Engerer2 Model, and γ is the solar elevation angle in a similar way as demonstrated in Ma Lu et al. (2022).

$$k_{diff_{PAR}} = \frac{(1+0.3\times(1-k_d^2))\times k_d}{1+(1-k_d^2)\times\cos^2(90^{\circ}-\gamma)\times\cos^3\gamma} \qquad \text{(eq. 9)}$$

With the $K_{diff_{Parr}}$, we can use the same relationships of the (eq. 1), (eq. 2) and (eq. 3) to calculate the PAR_{INC}, PAR_{DIRECT} and PAR_{DIFUSE}.

PV installation parameters

It's considered the same as the experimental site has, where is shown in Table 3.

Table 3: Equipment specification on Agrivoltaics Area

Equipment Traits	Equipment Specs
Tracking System	Single-Axis
Strings	4
Pier High	1.5 [meters]
GCR	31.47 %
Pitch	6.1 [meters]
Clearence	0.70 [meters]
Module	Canadian 385W bifacial

Direct and Diffuse Shading

Shading for the direct component (DNI) are considered with a binary relationship. An obstacle of height h casts a shadow effects with length L_S onto the pitch surface (eq. 10). The direct irradiance is thus defined as where d is the horizontal distance from the obstacle (eq. 11). For diffuse radiation (DHI), the shading is assessed using a geometric view factor (F_V), representing the fraction of sky obstructed (eq. 12).

$$Ls = \frac{h}{\tan{(\gamma)}} \qquad \text{(eq. 10)}$$

$$H(d) = \begin{cases} 0, & d \leq L_S \; (in\ shade) \\ 1, & d > L_S \; (sunlight) \end{cases} \qquad \text{(eq. 11)}$$

$$F_V = \frac{1}{A_S} \iint_{A_S} \iint_{A_{obs}} \frac{\cos{((90^\circ - \gamma)_S)} \times \cos{((90^\circ - \gamma)_O)}}{\pi \times r^2} dA_{obs} dA_S \qquad \text{(eq. 12)}$$

Finally, the PAR incident on each point of the pitch, corrected for shading effects, is expressed as (eq. 13).This integrated approach combines astronomical models, spectral decomposition, and geometric shading analysis, ensuring accurate estimations of PAR availability across the pitch.

$$PAR_{inc} = H(d) \times PAR_{direct} \times \cos(90^\circ - \gamma) + \mathrm{PAR_{diffuse}}(1 - \mathrm{F_V}) \qquad \text{(eq. 13)}$$

2.2. Crop Modelling Methodology

Crop yield modeling integrates detailed physiological processes and environmental conditions through a system of differential equations (eqs. 14 to 16) that simulate biomass accumulation and its allocation to plant organs, driven primarily by intercepted PAR and crop-specific Radiation Use Efficiency (RUE) across phenological stages as described by Breaudoin, N., et al. 2023. These stages are defined by cumulative Growing Degree Days (GDD), while Leaf Area Index (LAI) progression is explicitly modeled to capture canopy dynamics affecting light interception (k) as described by Jones, J.W., 2003 and Tappi, M. et al. 2023.

$$Daily\ Biomass = RUE * PAR * (1 - e^{-k*LAI}) \qquad \text{(eq. 14)}$$

$$Total\ Biomass = \sum_{i=1}^{n} Daily\ Biomass \qquad \text{(eq. 15)}$$

$$Crop_{yield} = Biomass * Harvest_{index} \qquad \text{(eq. 16)}$$

Photovoltaic shading effects are incorporated by adjusting radiation inputs and modifying microclimatic factors such as temperature and humidity, with evapotranspiration and water stress also accounted for (Zotarelli, L. 2013). This comprehensive framework enables accurate simulation of real-world conditions and supports validation through comparisons with experimental yield data under AgriPV scenarios.

3. Experimental Site and Equipment

Experiments were conducted in Sorocaba/SP, Brazil, from May to September 2023. The site included distinct areas dedicated to AgriPV and conventional agriculture controls, each covering approximately 500 m². Soybean crops were planted at densities of 250,000 and 300,000 plants per hectare, arranged in randomized blocks with six replicates per treatment and is shown on Figure 2A with a photo of the experiment site on Fig 2B the area sketch of the experiment. Initial irrigation was applied for crop establishment, transitioning to rainfed management afterward. The experimental AgriPV site specifications are shown on Table 3.

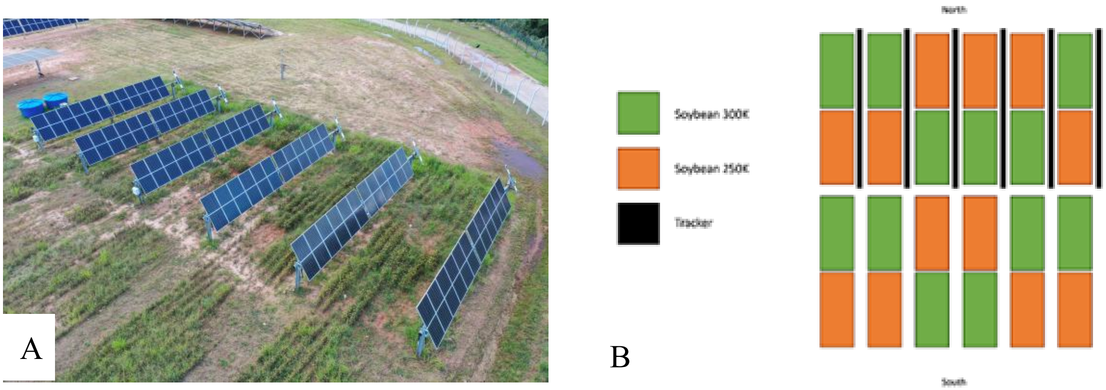

Figure 2: A) Aerial photograph of the experimental area. B) Sketch of the experimental area.

4. Results

The simulation based on the radiation model estimated the total Photosynthetically Active Radiation (PAR) over the cropping period, indicating that PAR accounted for 40.93% of the Global Horizontal Irradiance (GHI), as shown in Table 4. This proportion is notably lower than the standard 50% value commonly cited by Spitters et al. (1986), which aligns with expectations due to the inclusion of shading effects from photovoltaic (PV) modules in the model.

Table 4: Total TMY GHI (Wm-2), simulated PAR (Wm-2), measured and modelled soybean yield (gm-2) for the cropping period.

TMY GHI (Wm-2)	Simulated PAR from TMY (Wm-2)	Measured field yield (gm-2)	Modelled yield (gm-2)
780,420	319,457.60	143.17	156.79

The comparison between the measured and simulated soybean yields shows a difference of 8.68%, with the model slightly overestimating production. This level of deviation is consistent with the findings of Phoc, L. H., et al. 2023, who reported similar differences between observed and simulated yields in crop models and with Laub, M., 2022, who developed a different crop model system, but with similar results. The result indicates a good level of agreement between field observations and simulation outputs, supporting the validity of the radiation and crop modeling framework under AgriPV conditions. Minor discrepancies may be attributed to local microclimatic variations, soil conditions, or unmodeled biotic factors, which can influence field productivity but are not fully captured in the simulation.

The comparative analysis between measured and modeled PAR of the pitch throughout the day is presented in figure 3. As expected, slight differences are observed primarily due to non-linear factors such as atmospheric conditions, variations in cloud cover, aerosol concentration, and sensor calibration discrepancies. These factors introduce inherent variability in radiation measurement and modeling, contributing to minor deviations. Nonetheless, both measured and simulated values exhibit closely aligned patterns and magnitudes, demonstrating the robustness and reliability of the radiation modeling technique used in this study. The calculated Root Mean Square Error (RMSE) for the modeled PAR values against the measured values is 107.16 W/m². Additionally, the total daily PAR measured was 2,958.73 W/m² compared to the modeled total of 2,494.05 W/m², reflecting the model's accuracy in capturing daily radiation trends.

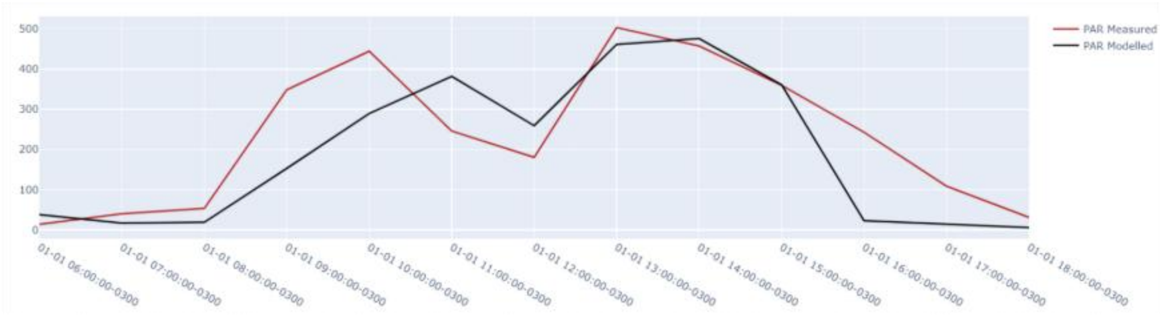

Figure 3: Comparison of measured and modeled PAR of the pitch.

5. Acknowledgments

The authors would like to express their sincere gratitude to FIT and Nextracker for their invaluable support and collaboration, which made this research possible. Their resources, expertise, and commitment to innovation provided the foundation for the successful completion of this study.

6. References

Anderson, K.S., Hansen, C.W., Holmgren, W.F., Jensen, A.R., Mikofski, M.A., Driesse, A., 2023. pvlib python: 2023 Project Update. Journal of Open Source Software 8, 5994.

Breaudoin, N., Lecharpentier, P., Ripoche-Wachter, D., Strullu, L., Mary, B., Léonard, J., Launay, M., Justes, E., 2023. Stics Soil Crop Model. Conceptual Framework, Equations and Uses, first ed. Quae, Versailles.

Bright, J.M., Engerer, N.A., 2019. Engerer2: Global re-parameterization, update, and validation of an irradiance separation model at different temporal resolutions. Journal of Renewable and Sustainable Energy 11, 033701.

Engerer, N.A., 2015. Minute resolution estimates of the diffuse fraction of global irradiance for southeastern Australia. Solar Energy, vol. 116, p. 215-237.

Gracia, A. M., Huld, T., 2013. Performance comparison of different models for the estimation of global irradiance on inclined surfaces: Validation of the model implemented in PVGIS. JRC Technical Report.

Huld, T., Paietta, E., Zangheri, P., Pinedo Pascua, I., 2018. Assembling Typical Meteorological Year Data Sets for Building Energy Performance Using Reanalysis and Satellite-Based Data. Atmosphere 9, 53.

Jones, J.W., Hoogenboom, G., Porter, C.H., Boote, K.J., Batchelor, W.D., Hunt, L.A., Wilkens, P.W., Singh, U., Gijsman, A.J., Ritchie, J.T., 2003. The DSSAT cropping system model. European Journal of Agronomy, 18, 235-265.

Laub, M., Pataczek, L., Feuerbacher, A., Zikeli, S., Högy, P., Contreras, S., 2022. Contrasting yield responses at varying levels of shade suggest different suitability of crops for dual land-use systems: a meta-analysis. Agronomy for Sustainable Development. 42, 51.

Ma Lu, S., Zainali, S., Stridh, B., Avelin, A., Amaducci, A., Colauzzi, M., Campana, P.E., 2022. Photosynthetically active radiation decomposition models for agrivoltaic systems applications.Solar Energy, vol. 244, pp. 536-549

Mikofski, M.A., Darawali, R., Hamer, M., Neubert, A., Newmiller, J., 2019. Bifacial Performance Modeling in Large Arrays. In: Proceedings of the 46th IEEE Photovoltaic Specialists Conference (PVSC), Chicago, IL, USA, pp. 1282–1287.

Phuoc, L.H., Suliansyah, I., Arlius, F., Chaniago, I., Xuan, N.T.T., Quang, P.V., 2023. Literature review crop modeling and introduction a simple crop model. Journal of Applied Agricultural Science and Technology 7, 197–216.

Reda, I., Andreas, A., 2004. Solar position algorithm for solar radiation applications. Solar Energy, vol. 76, no. 5, pp. 577-589.

Reda, I., Andreas, A., 2007. Corrigendum to Solar position algorithm for solar radiation applications. Solar Energy, vol. 81, no. 6, p. 838.

Spitters, C.J.T., Toussaint, H.A.J.M., Goudriaan, J., 1986. Separating the diffuse and direct component of global radiation and its implications for modeling canopy photosynthesis Part I. Components of incoming radiation. Agricultural and Forest Meteorology, vol. 38, no.1, pp. 217-229.

Tappi, M., Mazzocchi, C., Nocetti, D., Vieri, S., 2023. Crop varieties, phenological phases and the yield-weather relationship: Evidence from the Italian durum wheat production. Bio-based and Applied Economics.

Zotarelli, L., Dukes, M.D., Romero, C.C., Migliaccio, K.W., Morgan, K.T., 2013. Step by Step Calculation of the Penman-Monteith Evapotranspiration (FAO-56 Method). IFAS Extension, University of Florida, AE459.